Photogrammetrie • Fernerkundung • Geoinformation 4/2006, S. 303–314, 10 figs., 3 tabs.

Comparison of DSM Generation Methods on IKONOS Images

Thomas Krauß, Manfred Lehner, Peter Reinartz, Weßling & Uwe Stilla, München

Keywords: GeoInformatics, VHR data, Stereo Data, DSM generation, dynamic programming

Abstract: In this article two methods for an almost fully automatic generation of digital surface models (DSM) from Ikonos stereo data are described and limitations are analyzed. An important critical parameter for the derivation of DSM is the convergence angle of the stereo pair. Impacts of this value are shown and discussed.

Zusammenfassung: *Vergleich von DSM-Erstellungsmethoden auf Basis von IKONOS-Stereobildern*. In diesem Beitrag werden zwei Methoden für die nahezu vollautomatische Erzeugung digitaler Oberflächenmodelle (digital surface models, DSMs) beschrieben und analysiert. Ein wichtiger kritischer Parameter für die Gewinnung digitaler Oberflächenmodelle ist der Konvergenzwinkel der beiden Stereo-Aufnahmen. Der Einfluss dieses Parameters wird untersucht.

1 Introduction

Digital surface models (DSM) and three dimensional city models are important for many applications. Beside of maps, urban planning and information systems stereo data become essential in the case of catastrophes like earth quakes or floodings or in case of civil defense applications because they show the degree and the extent of destruction much more clearly than single images. An automatic interpretation of stereo images regarding exact location and height information will lead to fast change detection capabilities.

For this reason a system which is able to generate fully automatically DSMs and even 3D-city models from VHR satellite imagery like Ikonos is of great value for many applications. Since the intended purpose is to provide such models very quickly e. g. in disaster situations there are some requirements. A main point is that the information has to be gained in a short time for any possible acquisition area on the earth surface. Such constraints lead to the usage of stereo images from very high resolution (VHR) satellites from which the high resolution urban DSM can be derived. Beside this it is not possible to rely on locally available information like cadastral data or data of street networks in most developing countries. The models have to be generated fast with a reasonable accuracy for relatively large urban regions.

Two methods for an approach to a fully automatic generation of a DSM are described and limitations are analyzed. One critical parameter for the derivation of a DSM is the convergence angle of the stereo pair. Based on Ikonos stereo pairs with different convergence angles the impact of this value is examined and effects on the accuracy of the two methods are shown and discussed.

Three dimensional city models

Currently there exists a broad variety of methods for city modeling. These methods are mostly based on cadastral data, aerial images, aerial and terrestrial laser scanner

1432-8364/06/2006/0303 $ 3.00

data, terrestrial photographs and much more. The modeling integrates data from several of these sources in often intense manual work to the urban models (CyberCity 2006, 3D Geo 2006).

For example CyberCity uses a semi-automatic extraction of 3D-point-clouds on a photogrammetric workstation. From these points the roofs are generated and the walls are built by projection of the roofs to the digital terrain model or directly from cadastral data. The textures of roofs and walls are finally extracted by projection of the models into the aerial photos. As stated by CyberCity a good operator is able to extract up to 500 roof parts per day.

In our approach a big limitation is the missing availability of several data sources. To create models for a selected urban area of the world in a short time it is often only possible to obtain very few high resolution satellite images of the area.

Subject of this work is to develop a system which creates urban models only from a minimum of two high resolution stereo satellite images. Such images are provided at the moment e. g. by Space Imaging (Ikonos, SpaceImaging 2006) with a ground resolution of about 1 meter pan and 4 m multispectral or Digital Globe (QuickBird, 60 cm panchromatic and 2.4 m multispectral).
In the near future many more high resolution optical satellites are due to go into operation like WorldView I (2006) and II (2008) offering half-meter panchromatic and 1.4 to 1.8 m multispectral resolution (DigitalGlobe 2006).

Methods and algorithms

Area based matching algorithms depend on comparing similar areas of a matching window. But areas with steep slopes and large convergence angles lead to problems with occlusion where such area based matching fails.

One requirement for a good algorithm for generating DSMs in urban areas is therefore a good handling of geometric changes (a roof appearing wide in one and narrow in the other image) and occlusions (walls only seen in one image).

By visual interpretation of a stereo image pair, objects like houses, trees and cars can be interpreted easily. Also the human recognition masks out inconsistent areas as occlusions automatically. Hidden features in one and the other image vanish when looking at the stereoscopic image and the brain recognizes a fairly good 3D image with almost perfect height information.

Therefore an algorithm was searched which maps corresponding lines of the image pair one to the other. This restriction to lines only can be introduced in a first approch if we stick to epipolar geometry of the images.

A possible solution was found in an approach called "dynamic time warping" based on dynamic programming which is well known in speech recognition (Ney 1982, Sakoe & Chiba 1978, Itakura 1975). Recorded samples of words rarely fit to actual spoken words. A system has to match the recorded voice with learned words. To achieve this all samples are fragmented in overlapping short parts of which a spectral characteristic is memorized. The same procedure is applied to the voice input. As speech is varying in duration such sequences seldom fit together. But a simple linear stretch in time is not applicable because words are not uniformly stretched. Vowels are stretched more whereas consonants mostly keep the same length.

Due to the fact that the requirements are very comparable – warp two sequences of values to each other – this approach seems to be suitable. Similar algorithms are already used in the meantime also in computer vision (van Meerbergen et al. 2002, Hirschmüller 2005).

2 Description of the DSM generation methods

2.1 *Hierarchical intensitiy based matching (''method A'')*

Hierarchical intensity based matching as implemented into XDibias image processing system of DLR consists of two major steps.

In a first step the matching process uses a resolution pyramid (Lehner & Gill 1992, Kornus et al. 2000) to cope even with large stereo image distortions stemming from carrier movement and terrain. Large local parallaxes can be handled without knowledge of exterior orientation which is often not available with sufficient accuracy. The selection of pattern windows is based on the Foerstner interest operator (Foerstner & Guelch 1987) which is applied to one of the stereo partners. For selection of search areas in the other stereo partner(s) local affine transformations are estimated based on already available tie points in the neighborhood from a coarser level of the image pyramid.

Tie points with an accuracy of one pixel are located via the maximum of the normalized correlation coefficients computed by sliding the pattern area all over the search area. These approximate coordinates of tie points are refined to sub-pixel accuracy by local least squares matching (LSM). The number of tie points found and their final sub-pixel accuracy achieved depend mainly on image similarity and decrease with increasing stereo angles or time gaps between imaging. The software was originally devised for along-track 3-line stereo imaging as utilized by stereo scanners MEOSS and MOMS operated by DLR.

Normally, the procedure can be executed fully automatically and results in a rather sparse set of tie points well suited for introduction into bundle adjustment and as an excellent source of seed points for further densification via region growing in the second step. For example in the Munich Ikonos case there are only 1% tie points or 0.6% in Athens area when the totally available number of pixels is taken as reference.

The second step uses the region growing concept first published by Otto & Chau (1989) based on the implementation of the Technical University of Munich (TUM) (Heipke et al. 1996). It combines LSM with a strategy for local propagation of initial conditions of LSM.

Various methods for blunder reduction are used for both steps of the matching:

- Threshold for correlation coefficient
- 2-directional matching and threshold on resulting shifts of the coordinates
- Threshold on residuals in image space from forward intersection based on the rigorous modeling of the imaging process or on rational polynomial functions (RPC).

In areas of low contrast the propagation of affine transformation parameters for LSM in region growing leads to high rates of blunders. In order to avoid intrusion into homogeneous image areas (e. g. roof planes without structure) the extracted image chips are subject to low thresholds on variance and roundness of the Foerstner interest operator. This and the many occlusions found in densely built-up areas imaged with a large stereo angle create lots of insurmountable barriers for region growing. Thus for this type of stereo imagery the massive number of seed points provided by the matching in step one turns out to be essential for the success of the region growing.

The numbers of tie points found and their sub-pixel accuracy is highly dependent on the stereo angle. A large stereo angle and thus a large base to height ratio b/h leads to poorer numbers of tie points and to lower accuracy in LSM via increasing dissimilarity of correctly extracted image chips. Thus, a large b/h cannot be recommended for stereo imaging of city areas. This contradicts the normal imaging practice for Ikonos and QuickBird stereo acquisitions. Tab. 1 gives the percentages of tie points from the two matching steps for the Munich and Athens test areas.

Tab. 1: Percentages of tie points in relation to interest operator points (original image resolution of image pyramid) and total number of pixels in image (region growing).

Test area	Stereo angle (degrees)	b/h ratio	Percentage of tie points	
			Base: interest op.points	Base: total pixels
Munich	9.95°	0.17	86%	84%
Athens	30.28°	0.54	46%	41%

Tab. 2: Mean correlation coefficient c from LSM and standard deviation sigma of residuals in RPC forward intersection (after blunder reduction).

Area	c	sigma [pixel]
Munich	0.90	0.137
Athens	0.78	0.175

In a first approximation the standard deviation of stereo height measurement is proportional to the quotient of the standard deviation of the image coordinates from matching and the base to height ratio. Thus, a smaller b/h can be compensated by improved matching accuracy. This effect can be seen in Tab. 2 for our test areas where the smaller b/h seems to be even more than compensated by better matching conditions. Thus, in case of small stereo angles more tie points with overall better accuracy can be determined in densely built-up areas resulting in a better DSM.

The tie point determination described above does not require epipolar geometry. The method described in the next chapter is depending on epipolar geometry. For VHR satellite imagery software has been developed to derive quasi epipolar images using algorithms given in Morgan (2004). For standard stereo configurations Ikonos images can be ordered already in epipolar geometry from SpaceImaging. With the newly developed software epipolar images can be generated also for multi-temporal stereo pairs and non-standard Ikonos stereo imaging conditions as for Munich test case.

In order to compute a DSM from the tie point cloud from matching the object space coordinates of the tie points are computed by forward intersection based on the rigorous modeling of the imaging process or on RPC. If ground control points are available they are used in bundle adjustment or correction of RPC. The irregular 3D point cloud is transformed into a regular DSM grid by using the triangulation and interpolation as described in Hoja et al. (2005).

2.2 *Dynamic line warping (''method B'')*

The images are assumed to be available as a stereo pair with parallaxes in image line direction (epipolar images, horizontal epipolar lines). Creating a dense digital surface model (DSM) from such image pairs is based on finding corresponding image parts in each of the two images and calculating a local height of an image feature out of the relative displacement of the locations of this feature in the two images (parallaxes).

Because of the assumption of epipolar images there exist only horizontal parallaxes and no vertical shifts between the two images. This allows reducing the problem ''find correlations of image parts between two images'' to only ''find correlations in corresponding lines of the images''. Each line of an image is represented as a profile of gray values as shown in figure 1 top and bottom respectively.

Such sequences have to be mapped on each other stretching and compressing parts to achieve an optimal local fit. To achieve this the ''dynamic time warp'' algorithm used in speech recognition was implemented to warp image lines one to the other (Krauß et al. 2005).

The method used in speech recognition (Ney 1982) calculates spectral characteristics for short overlapping parts of the audio samples and distances between each of these parts and uses dynamic programming to receive a so called ''minimal total distance'' for the given sample with the compared sample of the dictionary. Only this minimum total distance is used further for determining the most probable sequence of words.

For explanation of the method let's take as an example two sequences of values I and I' as $I^T = (1\ 0\ 2\ 1\ 0)$ and $I'^T = (0\ 1\ 0\ 2\ 1)$. The distance-matrix $M_{i,j}$ will then be calculated as $M_{i,j} = |I_i - I'_j|$ thus

$$M = \begin{pmatrix} 1 & 0 & 1 & 1 & 0 \\ 0 & 1 & 0 & 2 & 1 \\ 2 & 1 & 2 & 0 & 1 \\ 1 & 0 & 1 & 1 & 0 \\ 0 & 1 & 0 & 2 & 1 \end{pmatrix}$$

In the next step the rows and columns are cumulated to a matrix D filling the first line and column according to

$$D_{1,j} = \sum_{k=1}^{j} M_{1,k}, \qquad D_{i,1} = \sum_{k=1}^{j} M_{k,1}$$

and the rest of the matrix $D_{i,j}(i,j > 1)$ as

$$D_{ij} = M_{ij} + \min\{D_{i-1,j}, D_{i,j-1}, D_{i-1,j-1}\}$$

yielding D in the example from above:

$$D = \begin{pmatrix} \mathbf{1} & \mathbf{1} & 2 & 3 & 3 \\ 1 & 2 & \mathbf{1} & 3 & 4 \\ 3 & 2 & 3 & \mathbf{1} & 2 \\ 4 & 2 & 3 & 2 & \mathbf{1} \\ 4 & 3 & 2 & 4 & \mathbf{2} \end{pmatrix}$$

In this Matrix D the overall distance is defined as the rightmost bottom element – in the example 2. This is a measure for all needed shifting, stretching and squeezing operations for one sequence to fit onto the other. In speech recognition it's sufficient finding the dictionary sample with the smallest minimal total distance to the given voice input. But beneath this minimal total distance a so called "minimal path" can be defined. This path connects the endpoints of the compared sequences in a manner describing what parts of one sequence has to be shifted, stretched or squeezed to fit on the other. From this minimal path the searched parallaxes can be extracted. Starting from the rightmost bottom element going back always using the smallest possible next neighbour to the top, left or top-left gives the minimal path (marked above in bold).

For the implementation of the algorithm we first have to define a "distance". In the case of a direct comparison of the sequences of gray values of the two epipolar images this can be in a first approach the absolute value of the gray value distance.

Calculating the matrix, picking a small area of the result and showing the extracted correlations between the input gray value profiles yields Fig. 1. As can be seen well areas with different widths in the profiles are correctly mapped to each other.

A perfectly diagonal line as minimal path represents no relative displacements between the two profiles. All deviations from this line indicate the searched parallaxes. If this minimal path is represented by pairs of coordinates $\mu_k = (i,j)_k$ it's possible to fit a parabola through $D_{i-1,j+1}$, $D_{i,j}$ and $D_{i+1,j-1}$ to calculate the parallaxes as the minimum of this parabola in subpixel accuracy.

Using small window areas of diameter ω around every line position for calculating the distance $M_{i,j}$ gives better results but introduces on the other hand smoothing effects as resulting from area based methods. The distance $M_{i,j}$ of line y with images $I_{x,y}$ and $I'_{x,y}$ and window size ω is then calculated as

$$M_{i,j} = \sum_{\lambda=-\lfloor\omega/2\rfloor}^{\omega-\lfloor\omega/2\rfloor-1} \sum_{\mu=-\lfloor\omega/2\rfloor}^{\omega-\lfloor\omega/2\rfloor-1} |I_{i+\lambda,y+\mu} - I'_{j+\lambda,y+\mu}|$$

Afterwards a vertical median filter of size 3 is applied to reduce line streaking and blunders resulting from the line by line correlation. For acceleration of processing time a maximum correlation window size can be chosen. Outside of this distance from the main diagonal the matrix M simply gets filled with a maximum distance value instead of the calculated distance.

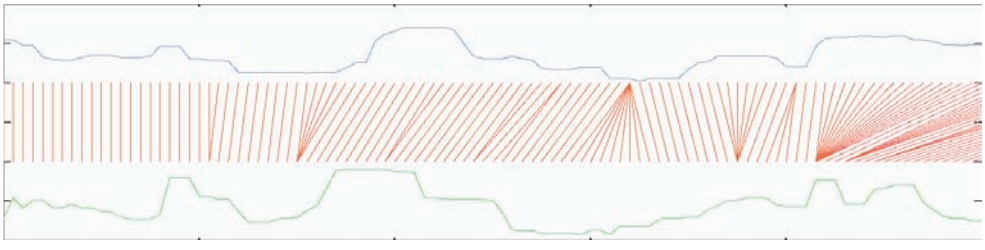

Fig. 1: Found correlations between the two input gray value profiles (top and bottom of graphic).

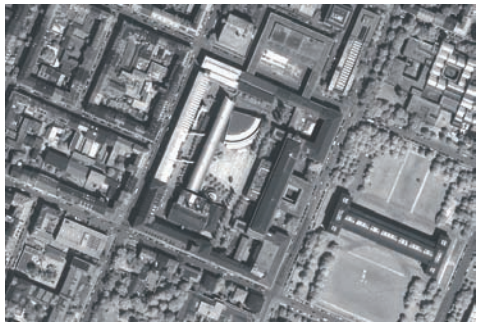

Fig. 2: Ikonos image of test area ''Munich TUM'' (600 m × 400 m).

3 Image and reference data

For experiments the following Ikonos data sets provided by Space Imaging were used:

- Munich acquired 2005-07-15, 10:28 GMT, level 1A images (only corrected for radiometry and inner orientation) with a ground resolution of 83 cm and declination angles of $+9.25^\circ$ and -4.45°
- Athens acquired 2004-07-24, 9:24 GMT, level 1B image pair (epipolar) with a ground resolution of 88 cm and declination angles of -19.99° and $+13.17^\circ$

Apart from these high resolution satellite imagery a set of laser scanner data from the region around the Technical University in Munich was available as reference data.

The high resolution Ikonos satellite imagery is accompanied by rational polynomial coefficients (RPCs) for every image. These coefficients are used to transform geographical coordinates longitude X, latitude Y and ellipsoid height Z to image coordinates $(x, y)^T$ by division of two polynoms with 20 coefficients each (Jacobsen et al. 2005, Grodecki et al. 2004).

The Munich scene is a non-standard Ikonos stereo acquisition with a small stereo angle of about only 10°. SpaceImaging provided the radiometrically corrected images with RPC. After applying the area based matching (image pyramid) tie points were available for transformation of the image pair into epipolar geometry (all parallaxes in column direction).

The Athens scene was acquired as a so called ''Ikonos standard stereo pair'' which stands for an exposure with declination angles of about 10° to 20° each in one orbit and delivery as epipolar images (actual stereo angle was 30.28°).

The images given in Fig. 3 contain the same clippings from the Ikonos stereo pair as the DSMs in Fig. 4. As can be seen the blocks of houses mostly contain narrow courtyards in the center. These courtyards are about 8 to 10 m wide whereas the houses

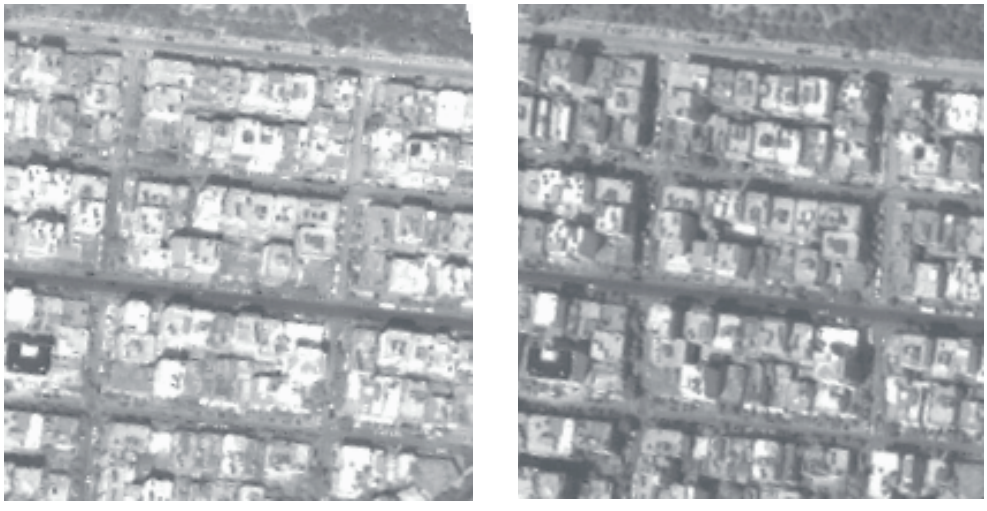

Fig. 3: Sections (250 m × 250 m) of the stereo pair test area ''Athens''.

are about 15 m and the streets are about 12 m wide.

4 Application of the methods to the test data

4.1 *Test data set Athens*

The first example is the test data set "Athens" as shown in Fig. 3. Applying first the classical hierarchical algorithm (referred as A in the following) gives as a result the DSM shown in Fig. 4, left.

Applying the dynamic programming algorithm (method B) with a window size $\omega = 3$ yields Fig. 4, right.

The DSM in Fig. 4, left generated with the classical hierarchical algorithm (A) shows no large blunders but a much more smooth DSM whereas the DSM calculated with the dynamic programming (method B, Fig. 4, right) shows sharp edges but many blunders and streaking in epipolar direction because of no linkage between the calculation of every epipolar line. As can be seen method B shows much more details especially at sharp ridges than method A but generates also more blunders.

As can be seen in Fig. 4 method A smoothes out most of the smaller courtyards because of the window size of 13×13 pixels used in region growing. The streets in this area are, however, wide enough to be found by method A. Method B on the other hand reveals sharp edges from top to bottom reproducing buildings, courtyards and streets much more clearly whereas the line streaking effects leading to blurry edges can be seen left to right – in epipolar direction.

4.2 *Test data set Munich*

Applying method A to the Munich scene shown in Fig. 2 yields the DSM shown in Fig. 5 and 6 left.

As can be seen the results are obviously better than in the Athens scene. Small courtyards are better resolved than in the previous test case. However comparing Fig. 5, left with the reference laser DSM (Fig. 7) shows some blurring at the edges of the buildings and smoothed out regions on the main building of the university.

After transforming the Munich scenes locally to epipolar geometry using some tie points the dynamic programming algorithm is applied to the area around the technical university with a window size of 3 (Fig. 5, right) and the analogous clipping in Fig. 6 on the right side.

Comparing the two DSMs generated by method A and B and the laser DSM reveils the differences as can be seen in Fig. 5 to 7.

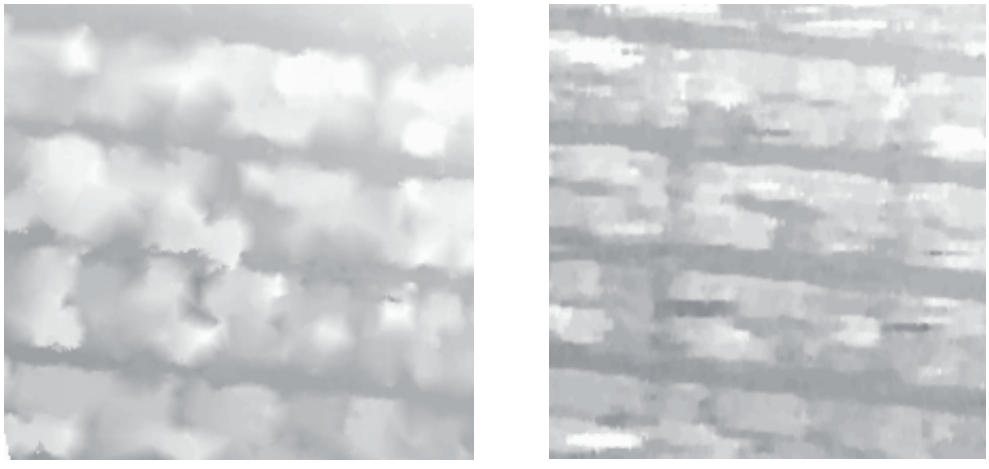

Fig. 4: Details of DSMs of the test area "Athens" (Fig. 3) generated by hierarchical intensity based matching (method A, left) and by dynamic line warping (method B, right).

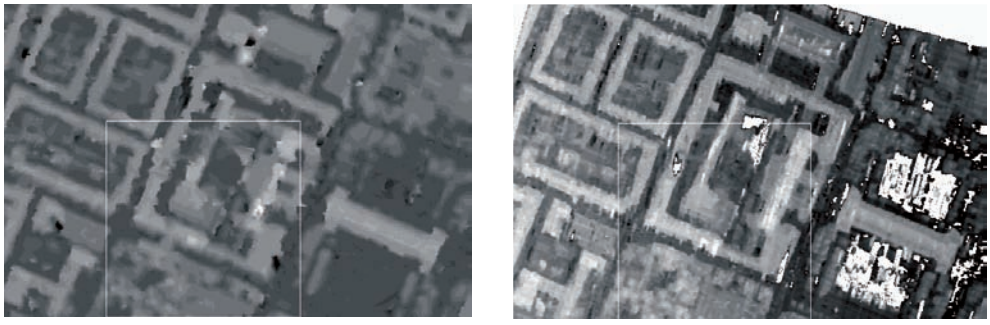

Fig. 5: DSM generated by applying the hierarchical intensity based matching of method A (left) to the Munich scene Fig. 2, right: DSM calculated with method B.

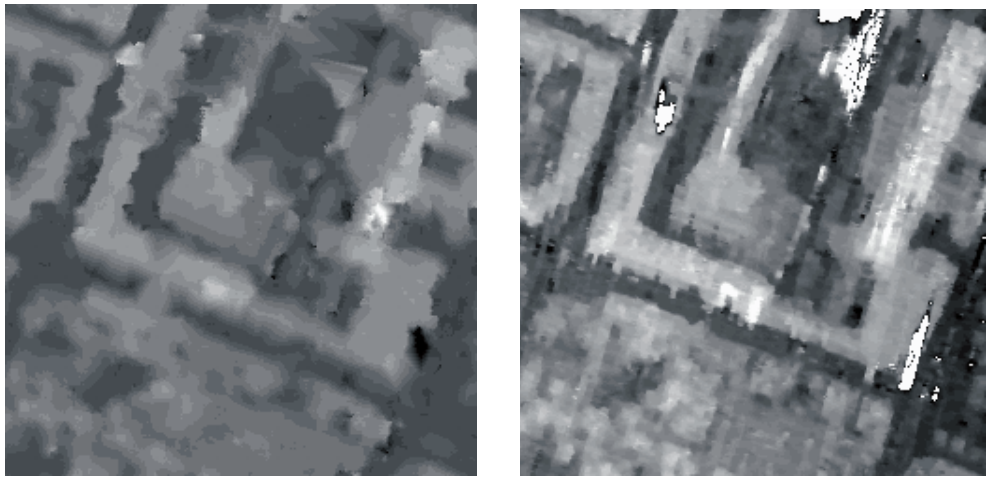

Fig. 6: Clips from Fig. 5, 250 m × 250 m, left method A, right method B.

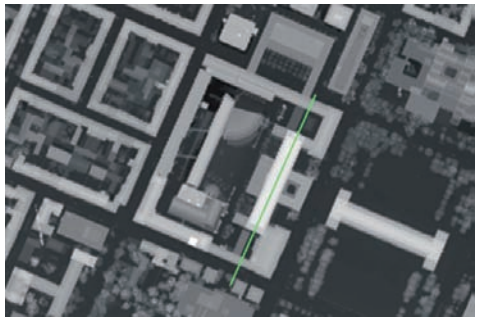

Fig. 7: DSM of test area ''Munich, TUM'' (Fig. 2) generated from Laser scanning data. The green line shows the location of the profile depicted in Fig. 9.

Fig. 7 shows the laser DSM used as reference data for comparison of the generated DSMs from the Ikonos images.

The DSM generated by method B shows much less smoothing than the one generated with method A but on the other hand more blunders as can be seen for example in the grass area near the Old Pinakothek and streaking effects in epipolar direction (top to bottom).

Fig. 8: Masks created manually showing buildings (left), streets, grass and soil (middle) and trees (right).

The edges of the buildings are more straight in epipolar direction with method B than with method A but cross epipolar direction more jagged than with method A due to the line streaking effects. So the tower of the university in the middle of the southern buildings gets nearly wiped out with method B due to the streaking where on the other hand the rim of the western building and the ridge of the main building is badly reproduced by method A.

5 Quality assessment of the generated DSMs

5.1 *Masking*

For assessment of the generated DSMs the test area is divided into three classes, namely:

- buildings
- streets, grass and soil
- trees

Masks for these areas were manually created (see Fig. 8).

Statistics and histograms were calculated for every class. Tab. 3 shows the mean heights h and standard deviation σ for each of the masked areas and each DSM case.

Tab. 3 shows that both methods estimate the heights of buildings in reference to the laser DSM about 2.5 m too low and the level of streets and soil about 1.5 m too high. This is due to a smoothing of the walls as can be seen also in the profile in Fig. 9 which raises on the one hand street levels in proximity to steep walls and lowers building heights near rims of the buildings on the other hand. The standard deviations of the differences certifies method A better results than method B especially in building areas.

Method B shows an overestimation of tree heights in comparison to the laser DSM and method A of about 4 m. The laser DSM is a composit of flight campaigns in April and November 2003 with sparse foliage and all fetched 3D points averaged. Thus the heights in the laser DSM should be lower than the DSMs generated from the july Ikonos imagery. As shown in Reinartz et al. (2005) forest and tree heights are often underestimated by optical stereo evaluation using method A.

Tab. 3: Mean heights h and standard deviation sigma in meters for the three masks applied to laser-DSM and DSMs generated by method A and B. The last two lines show the difference DSMs between the DSM of method A and the laser DSM and DSM B and the laser DSM.

	Buildings		Streets		Trees	
Channel	h	σ	h	σ	h	σ
Laser DSM	530.34	6.21	517.48	4.49	522.25	4.17
Method A	527.85	6.72	519.14	6.41	523.18	5.52
Method B	527.97	8.13	518.84	7.33	526.18	6.14
A − Laser	−2.49	3.49	1.66	5.56	0.92	4.68
B − Laser	−2.37	5.11	1.36	5.95	3.92	4.46

5.2 *Profiles*

As another method for visualization of the quality of two DSMs profiles are chosen. Fig. 9 shows a profile cut from south to north along the main building of the university starting at a tree south of the street and stretching over the campus through the street north as drawn into Fig. 7.

The first peak denotes a tree south of the street. The second peak is the first (southern) building, after a small courtyard follows the gable of the main building, a second yard and the northern building. Since the southern and northern buildings are cut across the roof slope can be seen.

Looking at the steep walls of the buildings a smoothing as shown in Fig. 9 on the right building can be seen. Analyzing the slope shows that the width of an object is almost correct at a height of about 80% and smoothes out about 4 to 5 meter at the bottom of a building.

In this case of the Munich scene no significant differences in smoothing out steep walls between method A and B can be seen. However both methods are not satisfactory enough because of large errors e. g. on the main building arising from missing tie points in method A or height errors in the first courtyard with method B arising from streaking effects in epipolar direction.

Looking at profiles across buildings in the Athens case gives another view as can be seen in Fig. 10.

The profile show a clear difference in the smoothing out of steep walls in comparison to the munich scene profiles above. Especially in Fig. 10 complete courtyards are missing due to non existing tie points because of the large convergence angle of this stereo pair.

The quality of the DSM generated by method B shows no such big degradation under increasing convergence angles as method A. Here also streets, courtyards and steep walls still remain visible and get reproduced reasonably good as can be proved by visual check of the DSMs from Fig. 4 with the original imagery in Fig. 3.

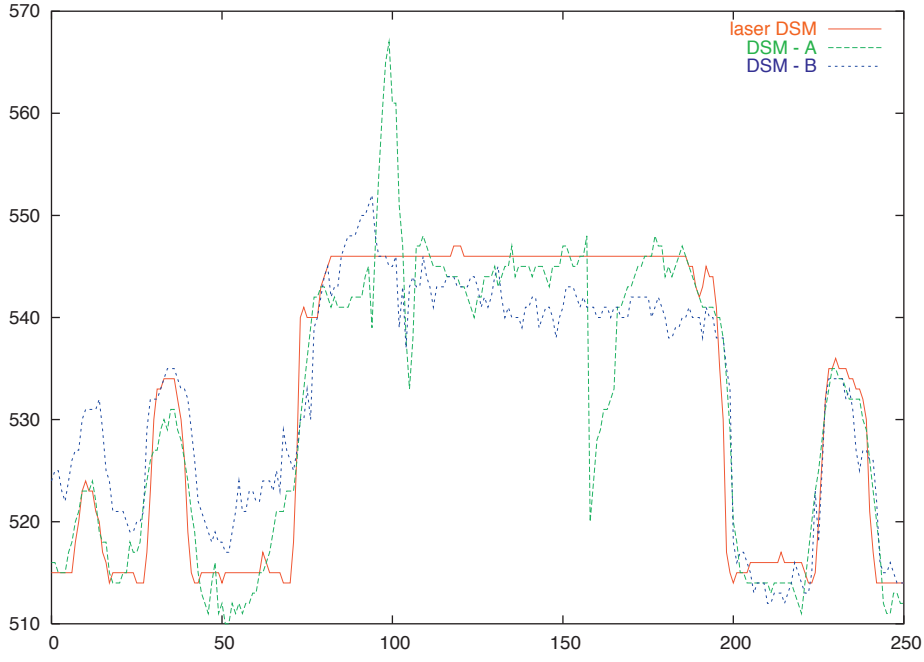

Fig. 9: Profiles of the DSMs generated by method A and B for test area ''Munich, TUM'' (all units in meter). The location of the profile is shown in Fig. 7.

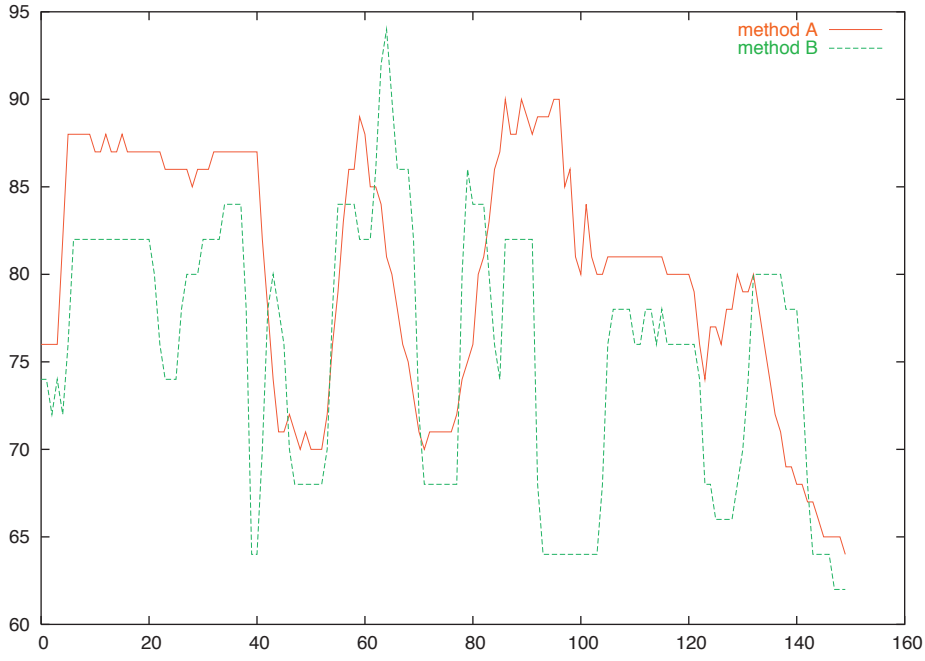

Fig. 10: Profile from center of Fig. 4 showing higher buildings with narrow courtyards.

6 Discussion

Comparing the DSMs generated by the two methods for the two test scenes shows pros and cons for both methods. So method A relies heavily on finding good tie points in the first step since the region growing can't proceed to large areas in urban scenes due to occlusion and other effects. But missing tie points result in a smoothing out and therefore no straight and sharp edges.

Method B on the other hand suffers in the herein presented algorithm much from streaking effects and large blunders in meadows.

But comparing the profiles of the DSMs of the Munich scene with the Athens scene shows clearly an effect of the larger convergence angle in the Athens case. While method B achieves almost the same character of the DSM as in the Munich case with a relatively small convergence angle the DSM quality of method A drops significantly due to more missing important tie points and therefore a smoothing out of much more small details like streets or courtyards.

Further work will be needed to reduce the streaking between lines through interconnection of the epipolar lines in the DSM generation with method B. Also analyzing and eliminating large blunders in grass areas possibly due to BRDF effects have to be implemented.

References

3D Geo, 2006: http://www.landxplorer.net/. (accessed 02/2006)

CyberCity, 2006: http://www.cybercity.tv/. (accessed 02/2006)

DigitalGlobe, 2006: http://www.digitalglobe.com/about/imaging.shtml. (accessed 02/2006)

SpaceImaging, 2006: http://www.spaceimaging.com/. (accessed 02/2006)

Foerstner, W. & Guelch, E., 1987: A Fast Operator for Detection and Precise Location of Distinct Points, Corners and Centres of Circular Features. – ISPRS Intercommission Workshop, Interlaken.

Grodecki, J., Dial, G. & Lutes, J., 2004: Mathematical Model for 3D feature extraction from multiple satellite images described by RPCs. – ASPRS Annual Conference Procee-dings, Denver, Colorado

Heipke, C., Kornus, W. & Pfannenstein, A., 1996: The evaluation of MEOSS airborne 3-line scanner imagery – processing chain and results. – Photogrammetric Engineering and Remote Sensing **62** (3): 293–299.

Hirschmüller, H., 2005: Accurate and efficient stereo processing by semi-global matching and mutual information. – IEEE Conference on Computer Vision and Pattern Recognition (CVPR).

Hoja, D., Reinartz, P. & Lehner, M., 2005: DSM generation from high resolution satellite imagery using additional information contained in existing DSM. – International Archives of the Photogrammetry, Remote Sensing and Spa-tial Information Sciences **36** (1/W3). ISPRS Workshop, Hannover

Itakura, F., 1975: Minimum prediction residual principle applied to speech recognition. – IEEE Trans. Acoust. Speech signal process ASSP **23:** 67–72.

Jacobsen, K., Büyüksalih, G. & Topan, H., 2005: Geometric Models for the orientation of high resolution optical satellite sensors. – International Archives of the Photogrammetry, Remote Sensing and Spatial Information Sciences **36** (1/W3). ISPRS Workshop, Hannover.

Kornus, W., Lehner, M. & Schroeder, M., 2000: Geometric inflight calibration by block adjustment using MOMS-2P 3-line-imagery of three intersecting stereo-strips. SFPT (Société Française de Photogrammétrie et Télédétection) **159:** 42–54.

Krauß, T., Reinartz, P., Lehner, M., Schroeder, M. & Stilla, U., 2005: DEM Generation from Very High Resolution Stereo Satellite Data in Urban Areas Using Dynamic Program-ming. – International Archives of the Photogrammetry, Remote Sensing and Spatial Information Sciences **36** (1/W3).

Lehner, M. & Gill, R., 1992: Semi-automatic derivation of digital elevation models from stereoscopic 3-line scanner data. – ISPRS 29 (B4): 68–75.

Morgan, M., 2004: Epipolar Resampling of Linear Array Scanner Scenes. – PhD thesis, University of Calgary, Canada. UCGE Reports Nr. 20193.

Ney, H., 1982: Dynamic programming as a technique for pattern recognition. – Proc. 6th Int. Conf. Pattern Recognition, pp. 1119–1125.

Otto, G. & Chau, T., 1989: Region growing algorithm for matching of terrain images. – Image and vision computing **7** (2): 83–94.

Reinartz, P., Müller, R., Hoja, D., Lehner, M. & Schroeder, M., 2005: Comparison and Fusion of DEM derived from SPOT-5 HRS and SRTM Data and Estimation of Forest Heights. – Proc. EARSeL workshop Special Interest Group 3D Remote Sensing, pp. 10 on CD-ROM

Sakoe, H. & Chiba, S., 1978: Dynamic programming algorithm optimization for spoken word recognition. – IEEE Trans. Acoust. Speech signal process, ASSP **26:** 43–49.

van Meerbergen, G., Vergauwen, M., Pollefeys, M. & van Gool, L., 2002: A hierarchical symmetric stereo algorithm using dynamic programming. – International Journal of Computer Vision **47** (1/2/3): 275–285.

Addresses of the authors:

Dipl.-Phys. Thomas Krauß,
e-mail: thomas.krauss@dlr.de

Dr. Manfred Lehner
e-mail: manfred.lehner@dlr.de

Dr. Peter Reinartz
e-mail: peter.reinartz@dlr.de

German Aerospace Center (DLR)
Remote Sensing Technology Institute
PO Box 1116, D-82230 Weßling, Germany

Prof. Dr. Uwe Stilla
e-mail: stilla@bv.tu-muenchen.de

Photogrammetry and Remote Sensing
Technische Universität München
Arcisstrasse 21, D-80333 München

Manuskript eingereicht: März 2006
Angenommen: April 2006